Histochem Cell Biol
DOI 10.1007/s00418-012-0969-5

ORIGINAL PAPER

Evidence for a partial epithelial–mesenchymal transition in postnatal stages of rat auditory organ morphogenesis

Nicolas Johnen · Marie-Emilie Francart · Nicolas Thelen · Marie Cloes · Marc Thiry

Accepted: 7 May 2012

Abstract The epithelial–mesenchymal transition (EMT) plays a crucial role in the differentiation of many tissues and organs. So far, an EMT was not detected in the development of the auditory organ. To determine whether an EMT may play a role in the morphogenesis of the auditory organ, we studied the spatial localization of several EMT markers, the cell–cell adhesion molecules and intermediate filament cytoskeletal proteins, in epithelium of the dorsal cochlea during development of the rat Corti organ from E18 (18th embryonic day) until P25 (25th postnatal day). We examined by confocal microscopy immunolabelings on cryosections of whole cochleae with antibodies anti-cytokeratins as well as with antibodies anti-vimentin, anti-E-cadherin and anti-β-catenin. Our results showed a partial loss of E-cadherin and β-catenin and a temporary appearance of vimentin in pillar cells and Deiters between P8 and P10. These observations suggest that a partial EMT might be involved in the remodelling of the Corti organ during the postnatal stages of development in rat.

Keywords EMT · Cytoskeleton · Organ of Corti · Development

Electronic supplementary material The online version of this article (doi:10.1007/s00418-012-0969-5) contains supplementary material, which is available to authorized users.

N. Johnen (✉) · M.-E. Francart · N. Thelen · M. Cloes · M. Thiry
Department of Life Sciences, GIGA-Neurosciences, Unit of Cell and Tissue Biology, University of Liege, Avenue de l'hôpital 1, 4000 Liege, Belgium
e-mail: n.johnen@ulg.ac.be

M. Thiry
e-mail: mthiry@ulg.ac.be

Introduction

An epithelial–mesenchymal transition (EMT) is a biological process that allows a polarized epithelial cell to undergo multiple biochemical changes that enable it to assume a mesenchymal cell phenotype (Kalluri and Weinberg 2009; Savagner 2010; Thiery et al. 2009). During this process, epithelial cells loosen cell–cell adhesion, module their polarity and rearrange their cytoskeleton: intermediate filaments typically switch from cytokeratin to vimentin. They also enhance their motility capacity. The EMT plays key roles in the formation of the body plan and in the differentiation of multiple tissues and organs but it is also involved in tissue repair, tissue homeostasis, fibrosis, and carcinoma progression (Thiery et al. 2009).

Until now, EMT has been rarely mentioned in the inner ear organogenesis. In chick, EMT has been reported as a possible mechanism of semicircular canal morphogenesis (Kobayashi et al. 2008). More recently, an in vitro study has also indicated that sensory epithelial cells from mouse utricle can undergo an EMT to become cells expressing features of prosensory cells (Zhang and Hu 2012). By contrast, EMT has never been observed during auditory organ morphogenesis.

Auditory perception in mammals is mediated through a sensory epithelium, known as the organ of Corti (OC), located within the coiled cochlea in the ventral region of the inner ear (Kelley 2006; Kelley et al. 2009; Sato et al. 1999). The OC composed of two basic cell types: mechanosensory hair cells and nonsensory supporting cells. Hair cells are arranged into a single row of inner hair cells and three rows of outer hair cells. The population of supporting cells includes several highly specialised cell types: inner pillar cells, outer pillar cells, Deiters cells and phalangeal cells. These cells are arranged in a regular mosaic pattern running along the length of the snail-like cochlea from base to apex. The inner pillar

Published online: 19 May 2012

cells and outer pillar cells combine to form the tunnel of Corti, a fluid filled triangular space that separates the single row of inner hair cells from the first row of outer hair cells. The Nuel spaces are another interval in the OC that is situated between the outer pillar cells and the different rows of outer hair cells and Deiters cells.

The establishment of the OC is complex and the molecular mechanisms permitting its development are still little known (Mu et al. 1997; Kelley 2007). In rats, the OC grows up between E16 (16th embryonic day) and E18 from a band of epithelial cells located on the dorsal face of the cochlear duct (Thelen et al. 2009). This band of cells engaged in the development of the auditory organ has been also called zone of non-proliferating cells (ZNPC) because it is specifically labelled by $p27^{Kip1}$, a cyclin-dependent kinase (CDK) inhibitor (Chen and Segil 1999). The different cells of the Corti organ are in place at E18 (Thelen et al. 2009). However, its development will be achieved around P25 (25th postnatal day) (Whitlon 1993). The most conspicuous maturational changes take place before P12 (Roth and Bruns 1992a, b). These changes are the formation of the Corti tunnel, of the Nuel spaces and the change in cell shape of the hair cells. Concomitantly to these striking changes that require profound cellular rearrangements, a loss of E-cadherin on the lateral surfaces of pillar, outer hair and, Deiters cells which lie adjacent to fluid spaces has been reported in mouse from P7 (Whitlon 1993). Likewise, a presence of vimentin has been detected in OC during mouse prenatal (Wikstrom et al. 1988) and rat postnatal (Kuijpers et al. 1992) developmental stages. Together these data suggest that an EMT could be involved in the OC development.

In order to know whether an EMT plays a role in the auditory organ morphogenesis, we investigated the spatial localization of different EMT markers, cell–cell adhesive molecules and intermediate filaments, in the dorsal epithelium of the cochlea during the development of Corti organ in rat from E18 up to P25. We analysed by confocal microscopy immunolabelings on entire cochlea's cryosections with various anti-cytokeratin antibodies as well as antibodies anti-vimentin, anti-E-cadherin and anti-β-catenin. Our results show a partial loss of E-cadherin and β-catenin and a temporary appearance of vimentin in pillar cells and Deiters cells between P8 and P12. These observations suggest that a partial EMT may be responsible for opening of Corti tunnel and Nuel spaces.

Materials and methods

Animals and OC explants

Animal handling was carried out in compliance with the University of Liège Animal Care and Use Committee guidelines that are in accordance with the declaration of Helsinki. Wistar rats were bred in our animal facility. Time-mated pregnant Wistar rats were killed from E18 to P25. The day of coitus was recorded as day 0 of gestation. Embryos were removed from the uterus and transferred into a glass Petri dish containing 0.1 M Sörensen's buffer (0.1 M NaH_2PO_4, 0.1 M Na_2HPO_4, pH 7.4). Watchmaker forceps were used to dissect the cochleae under a stereomicroscope. The cochleas were then isolated, free from surrounding tissues.

Protein extraction and western blots

The rat tissue (cochlea, liver and lung) was homogenised in lysis buffer [20 mM Tris, 150 mM NaCl, 2 mM EGTA, 0.1 % (v/v) Triton X-100 and complete protease inhibitor cocktail (Roche, Brussels, Belgium)] with a sonicator (Sonics and materials, Danbury, UK) for 5–10 s at 4 °C of power 375 W 10–20 kHz. Extractions are incubated for 30 min at 4 °C then centrifuged at 12,000×g for 10 min. This step allowed the recovery of proteins in the supernatant.

Equivalent amounts of extracted proteins were loaded on each lane of a 12 % sodium dodecyl sulphate–polyacrylamide gel. After electrophoresis, proteins were transferred onto Hybond©-LFP transfer membrane (GE Healthcare, Amersham bioscience, New Jersey, USA). After blocking in 3 % nonfat milk in Tris-buffered saline Tween, the membrane was incubated with primary antibody overnight at 4 °C and then with a secondary antibody for 1 h at room temperature. Immunoreactive signals were visualised by enhanced fluorescent (Typhoon 9400, GE Healthcare, Amersham bioscience, New Jersey, USA). Primary antibodies used were: anti-vimentin mouse monoclonal IgG (1:250 dilution; Sigma Chemical Co., St. Louis, USA), anti-E-cadherin rabbit polyclonal IgG (1:100 dilution; Abcam, Cambridge, UK), anti-cytokeratin 8 (CK8) chicken polyclonal IgY (1:250 dilution; Abcam, Cambridge, UK), anti-β-catenin rabbit monoclonal IgG antibodies (1:125 dilution; Abcam, Cambridge, UK) anti-β-actin rabbit monoclonal IgG antibodies (1:1,000 dilution; Sigma Chemical Co., St. Louis, USA). Secondary antibodies were fluorescein (FITC) donkey anti-mouse IgG (Jackson ImmunoResearch, Suffolk, UK), rhodamine Red-X donkey anti-Rabbit IgG (Jackson immunoresearch, Suffolk, UK) and rhodamine Red-X donkey anti-chicken IgY (Jackson immunoresearch, Suffolk, UK) used at 1:2,500 (see supplemental data Fig. S1).

Preparation of OC for examination by light microscopy

The cochleas were fixed for 60 min at 4 °C in a solution composed of 2.5 % glutaraldehyde in 0.1 M Sörensen's buffer. After several washes in the same buffer, the

samples were then postfixed for 60 min with 2 % osmium tetroxide, washed in deionized water, dehydrated through graded ethanol (70, 95, 100 %), and embedded in Epon for 24–48 h at 60 °C. Semithin sections (1 µm thick) were obtained by means of an ultramicrotome (Reichert Ultracut E) equipped with a diamond knife. They were stained with 0.5 % toluidine blue in 1 % carbonate sodium and examined under an Olympus FSX100 microscope.

Immunocytochemistry

The cochleas were fixed for 60 min at 4 °C in a solution composed of 4 % formaldehyde in Sörensen's buffer (pH 7.4). After several washes in the same buffer, the samples were incubated in five baths of 30 % saccharose in Sörensen's buffer (20 min each), embedded in gelatin 7.5 %, sucrose 15 % and Sörensen's buffer mix for 15 min at 30 °C, and plunged into an isopentane bath on dry ice. Cryosections (14 or 30 µm thick) were obtained by means of a cryostat (Microm HM 560, Prosan).

For immunolabeling, cryosections were rinsed in PBS (140 mM NaCl, 2.6 mM KCl, 1.5 mM KH_2PO_4, 16 mM Na_2HPO_4, pH 7.4) and permeabilized for 10 min at room temperature in 1 % Triton X-100 in PBS. After being washed in PBS, the sections were soaked for 30 min at 37 °C in 10 % normal goat serum (NGS) in PBS, immersed for 30 min at 37 °C in the primary antibody containing 5 % NGS, washed in PBS, and immersed for 30 min at 37 °C in the secondary antibody. Finally, the cryosections were rinsed in PBS and mounted with Citifluor AF1 (Laborimpex, Brussels, Belgium). The primary antibodies were: anti-$p27^{kip1}$ mouse monoclonal IgG (1:100 dilution; Sigma Chemical Co., St. Louis, USA), anti-myosin VI rabbit monoclonal IgG (1:150 dilution; Sigma Chemical Co., St. Louis, USA), anti-vimentin mouse monoclonal IgG (1:100 dilution; Sigma Chemical Co., St. Louis, USA), anti-E cadherin rabbit polyclonal IgG (1:100 dilution; Abcam, Cambridge, UK;), anti-Cytokeratin-Pan mouse monoclonal IgG (1:100; Sigma, St. Louis, USA), anti-Cytokeratin 4 rabbit polyclonal IgG (1:100; Abcam, Cambridge, UK), anti-Cytokeratin 5 rabbit monoclonal IgG (1:100; Abcam, Cambridge, UK), anti-Cytokeratin 7 mouse monoclonal IgG (1:100 dilution; Abcam, Cambridge, UK), anti-Cytokeratin 8 (CK8) chicken polyclonal IgY (1:100 dilution; Abcam, Cambridge, UK) and anti-β-catenin rabbit monoclonal IgG antibodies (1:200 dilution; Abcam, Cambridge, UK). Specificities of different primary antibodies were summarised in Table S1 and in Fig. S1 (see supplemental data). The secondary antibodies used were: goat anti-mouse Alexa Fluor 488 (1:250 dilution; Molecular Probes, Leiden, The Netherlands; $h\upsilon_{ex}$ 495 nm/$h\upsilon_{em}$ 519 nm), goat anti-rabbit Alexa Fluor 594 (1:250 dilution; Molecular Probes, Leiden, The Netherlands; $h\upsilon_{ex}$ 590 nm/$h\upsilon_{em}$ 617 nm) and goat anti-chicken Alexa Fluor 594 (1:250 dilution; Molecular Probes, Leiden, The Netherlands; $h\upsilon_{ex}$ 590 nm/$h\upsilon_{em}$ 617 nm). In some case, we used DAPI (1:50,000 dilution; 4′,6-DiAmidino-2-PhenyIndole; Sigma, St. Louis, USA; $h\upsilon_{ex}$ 372 nm/$h\upsilon_{em}$ 456 nm) to visualise the cell nuclei. As a negative control, the primary antibody was omitted. In each case, no labelling occurred.

Slides were examined under an IX71 confocal microscope (Olympus). Acquisitions were made using either a ×40 or a ×60 objective. Optical sections were analysed with softwares FV10-ASW 3.0 Viewer (Olympus) and Imaris (Biplane Scientific). All images are single sections.

Results

Morphological analysis of OC development from E18 to P25 in rat

To successively follow the different steps of the OC formation in the cochlear canal, we have examined semithin sections in the base of samples taken in rat embryos aged from 18 to 22 days and in newborn rats aged from 0 to 25 days (Fig. 1a–o). In the Fig. 1, as in the following figures, we have shown that the developmental stages exhibiting the most interesting results.

At E18 (Fig. 1a), the cochlear duct is lined with a pseudostratified epithelium. We observe a depression separating the dorsal epithelium in two parts: the GER, on the modiolar side, in continuity with the future Reissner membrane, and the LER, on the striolar side, in continuity with the future stria vascularis. It is interesting to note that, at this stage, the scala tympani and vestibuli are not formed yet.

From E20 (Fig. 1b), the different cell types of the OC are in place. The inner hair cells, outer hair cells, pillar cells and Deiters cells are clearly recognisable. At P0 (Fig. 1d), the outer sulcus becomes a monostratified epithelium whereas the inner sulcus remains a pseudostratified epithelium. At this stage, the scala tympani and vestibuli are obvious.

At P8 (Fig. 1h), the tunnel of Corti and the Nuel spaces start to open. These fluid spaces will continue to enlarge until P25 (Fig. 1h–o) from the Corti tunnel to the modiolar side of the OC. Concomitantly to the opening of the fluid spaces, the OC, including the hair cells and the supporting cells, raises. At P10 (Fig. 1i), the inner sulcus becomes a monostratified epithelium.

Partial loss of E-cadherin between the pillar cells and between the Deiters' cells from P8

To determine whether a loss of cell–cell adhesion occurs during the OC morphogenesis, we realised immunolabellings

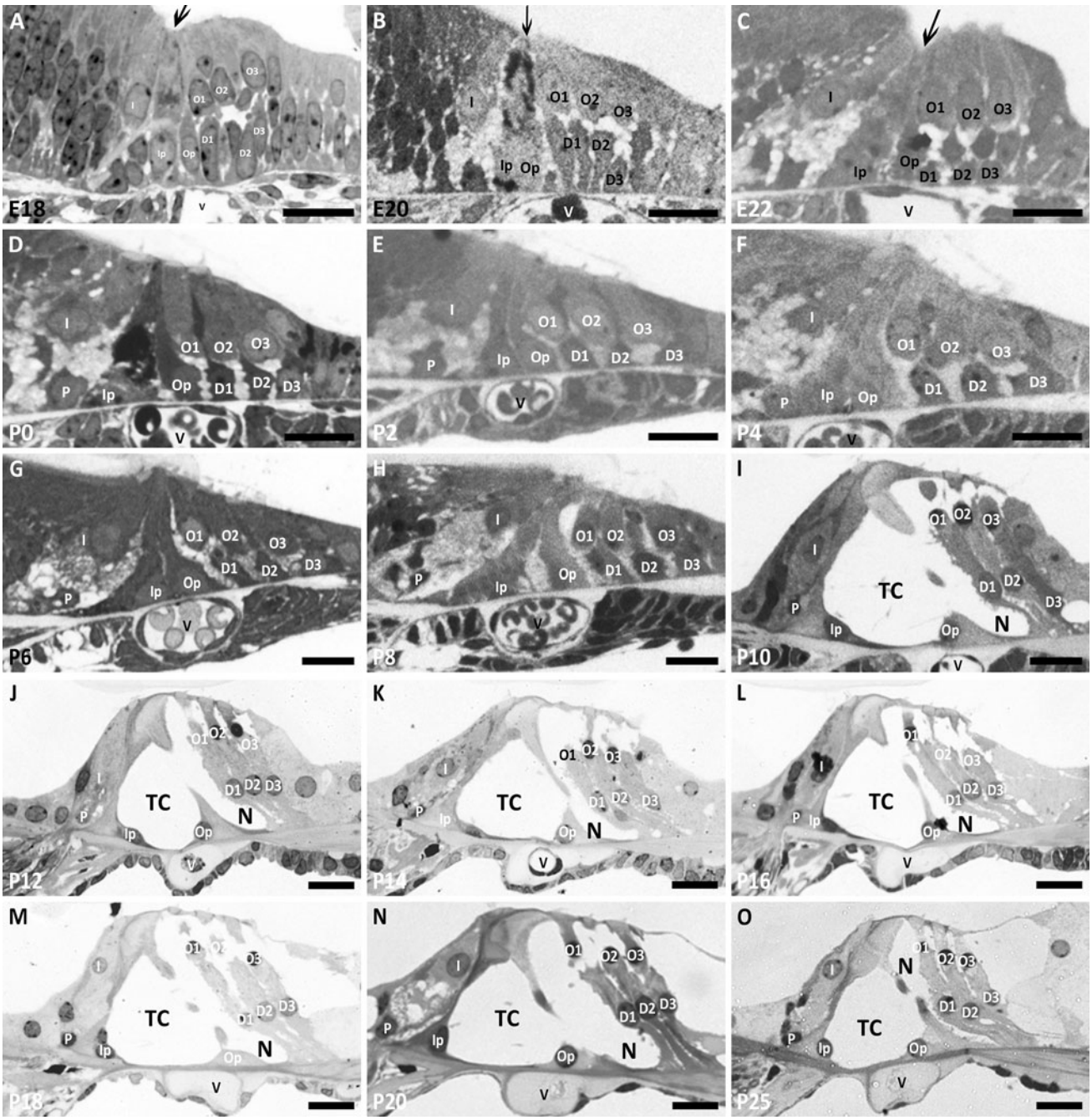

Fig. 1 Morphological analysis of the dorsal epithelium of the cochlear duct from E18 to P25 (**a**–**o**). All sections are stained with toluidine blue, oriented in the same way (*left* modiolar region, *bottom* dorsal wall of the cochlear duct) and corresponded to the basal region of the cochlea. *Arrows* indicate a depression of the dorsal epithelium, *D*(*1–3*) Deiters' cell, GER greater epithelial ridge, *I* inner hair cell, *Ip* inner pillar cell, *N* Nuel's space, *O*(*1–3*) outer hair cell, *Op* outer pillar cell, *P* phalangeal cell, *TC* Tunnel of Corti, *V* spiral vessel. *Bars* 10 μm

on entire cochlear cryosections with antibody anti-E-cadherin (Fig. 2a–f).

Under these experimental conditions, the E-cadherin labelling is exclusively detected in the epithelial cells (Fig. S2). The pattern of immunoreactivity was identical with that previously observed in rat (Simonneau et al. 2003). The E-cadherin labelling is found mainly in the external part of the OC whatever the developmental stages studied. The inner pillar cells are also E-cadherin-positive for all the developmental stages examined. The labelling is

observed on the lateral surfaces of cell membrane between the pillar cells and between the Deiters cells and their hair cells.

From E18 to P6 (Fig. 2a, b), we observe an intense labelling within the auditory epithelium except for the cells in the inner hair cell region. The labelling is particularly obvious between inner and outer pillar cells, between Deiters cells and their outer hair cells.

From P8 to P25 (Fig. 2c–f), when the tunnel of Corti and the Nuel spaces are opened, E-cadherin is retained only by those parts of the cells that are still in contact. Inside the inner and outer pillar cells and the Deiters cells, only their heads and their bases are E-cadherin positive.

To better demonstrate the loss of E-cadherin labelling between the inner and outer pillar cells, we have compared the OC labelling observed in longitudinal axis at P6, P10 and P16 (Fig. 3a–c). At P6 (Fig. 3a), an evident E-cadherin labelling is present all along the contact surface between the inner and outer pillar cells. At P10–16 (Fig. 3b, c), a reduction of E-cadherin labelling is observed on the lateral surfaces of cell membranes between inner and outer pillar cells which come in contact with the tunnel of Corti. By contrast, the apical surfaces of outer pillar cells, which are covered with the inner pillar cells, are strongly E-Cadherin-positive. A labelling also persists between the inner pillar cells and between the inner pillar cells and their adjacent phalangeal cells. The same reduction of labelling can be seen between the outer pillar cells and the first row of Deiters cells when the Nuel spaces open.

Loss of β-catenin in supporting cells of the OC from P12

In addition to E-cadherin, we have also studied the spatio-temporal localization of the cadherin-linked molecule β-catenin during OC morphogenesis (Fig. 4a–f).

We observe that all the epithelial cells are β-catenin-positive (Fig. S2). This is in total agreement with a previous study in rat (Simonneau et al. 2003). As previously reported (Kim et al. 1998), a β-catenin labelling is further found in the mesenchymal cells of the basilar membrane.

From E18 to P10, β-catenin is detected in all the epithelial cells of the cochlea duct, including the cells of the OC and the inner and outer sulcus (Fig. 4a–d). The labelling is essentially localized on the lateral surfaces of cell membranes. At P10, the fluorescent signal becomes more pronounced on the apical surfaces of outer pillar cells which are covered with the inner pillar cells (Fig. 4d).

From P12 to P25, the labelling of supporting cells situated in the external part of the OC reduces. This signal reduction is already well visible in the outer pillar cells at P12 (Fig. 4e). An attenuation of the fluorescent signal is also found in the inner pillar cells from the 14th day after birth. At this stage, an intense fluorescent spot is present in the Deiters cells under their outer hair cell. At P25, the labelling of Deiters cells is restricted to small spots at the lateral edges, near to the apical surfaces, which are in contact with their outer hair cells, and to large spots under their outer hair cells (Fig. 4f).

To know whether epithelial cells from the OC undergo a remodelling of their cytoskeleton, and in particular of their intermediate filaments, during development, we study the spatial-temporal localization of cytokeratins and vimentin on cryosections of rat cochlea from E18 to P25. We use an antibody against vimentin and various antibodies directed against cytokeratins: anti-cytokeratin pan (recognising cytokeratin 1, 4, 5, 6, 8, 10, 13, 18 and 19), anti-cytokeratin 4, anti-cytokeratin 5, anti-cytokeratin 7, and anti-cytokeratin 8. To identify the different cell types of the embryological and postnatal epithelium, double labellings are realised either with myosin VI, early marker and typical of the hair cells, or with p27kip1, marker specific for the supporting cells present in the ZNPC.

Temporary presence of vimentin in pillar and Deiters cells at P8–10

Independent of the developmental stage analysed, a vimentin labelling is found in the basilar membrane, the endothelium of the spiral vessel and the cartilaginous cells (Fig. S2). By contrast, no signal is revealed in nervous cells of the spiral ganglia with this antibody. The pattern of immunoreactivity was identical to that previously observed in rat (Osborn et al. 1984). In the OC, only the supporting cells can be vimentin-positive, hair cells are never labelled.

Before birth (Fig. 5a), vimentin is detected essentially in the future basilar membrane, the future Reissner membrane and the future stria vascularis. A very weak labelling is also found in the external part of the OC and in the cells of outer sulcus.

Between P0 and P6 (Fig. 5b), the labelling is localized preferentially in the basal part of the phalangeal cell, the pillar cells, especially the inner pillar cells, and the Deiters cells. The cells of the inner and outer sulcus are also labelled.

Between P8 and P10 (Fig. 5c, d), a strong signal intensity is obvious in the OC. In addition to an intense labelling of the basal region in all supporting cells, a diffuse labelling is also present through all their cytoplasm.

From P12 to P25 (Fig. 5e, f), the labelling decreases and finishes to disappear in the supporting cells of the OC. At P12 (Fig. 5e), the vimentin labelling appears to be structured in fibres situated on the whole height of the pillar cells. At P16, the basal parts of the phalangeal and Deiters cells are still labelled (Fig. 5f).

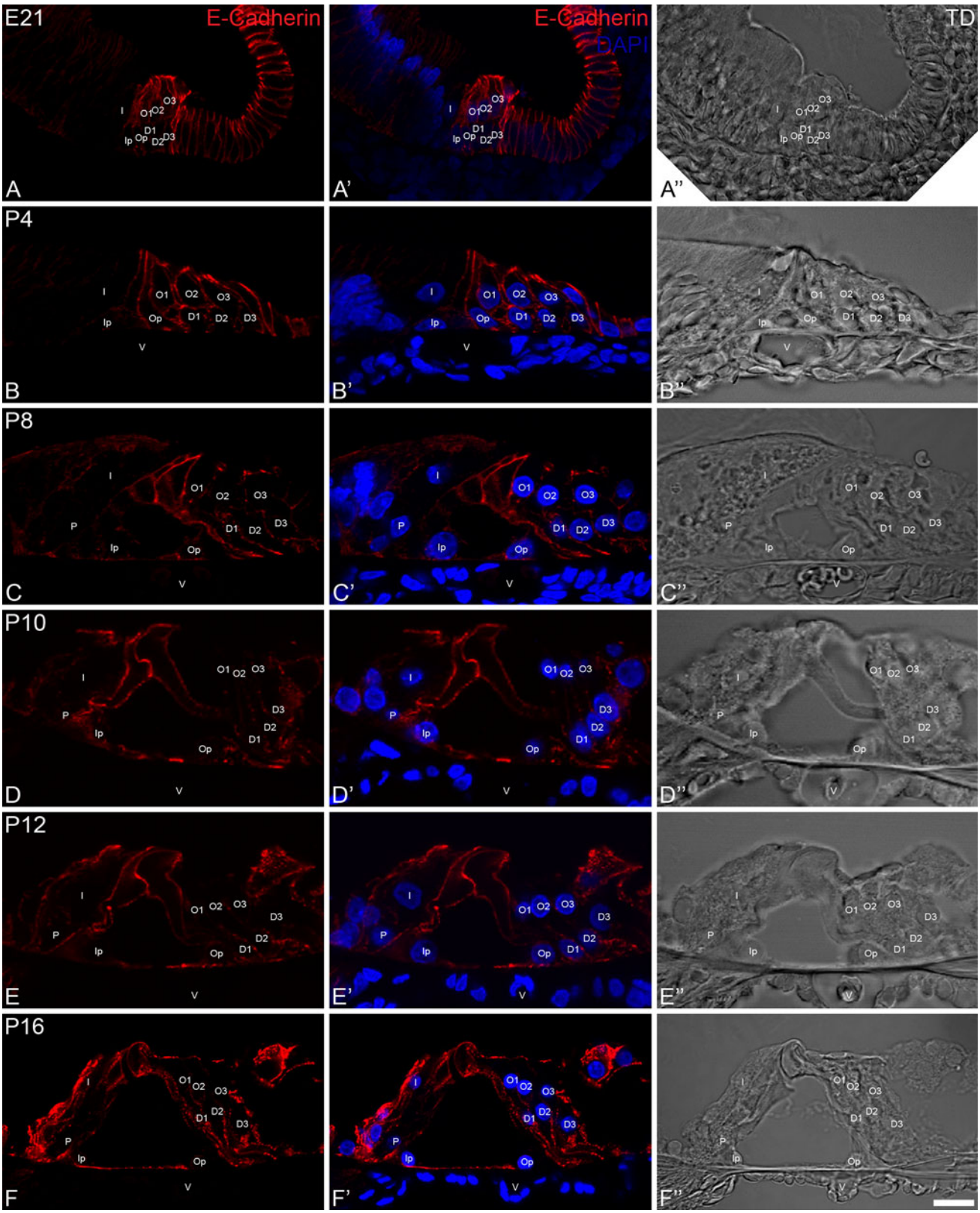

Fig. 2 E-Cadherin immunolabelling within the dorsal epithelium of the cochlear duct from E21 to P16. **a**–**f** Immunolocalization of the E-Cadherin (*red*). **a′**–**f′** Merged image with cell nuclei stained with DAPI (*blue*). **a″**–**f″** Visualisation of the OC by transmission detector. *D*(*1*–*3*) Deiters' cell, *Ip* inner pillar cell, *I* inner hair cell, *N* Nuel's spaces, *O*(*1*–*3*) outer hair cell, *Op* outer pillar cell, *P* phalangeal cell, *TC* tunnel of Corti, *V* spiral vessel. *Bar* 10 μm

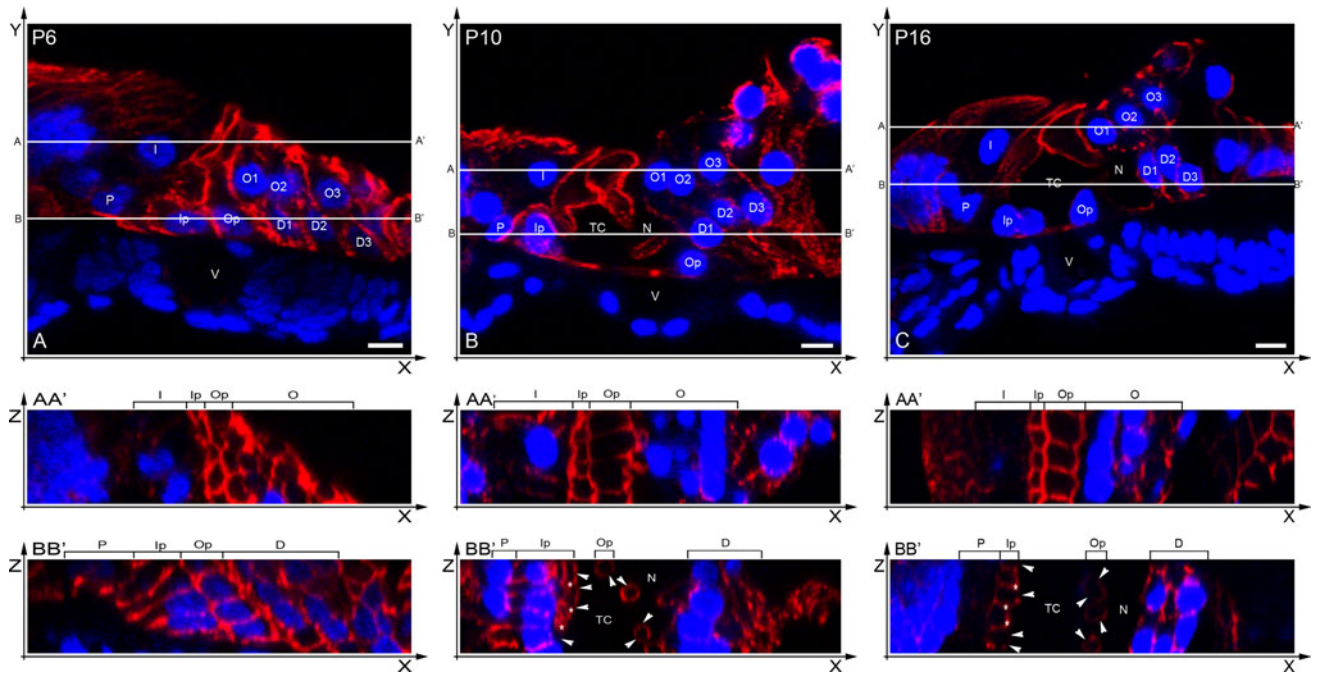

Fig. 3 E-Cadherin immunolabelling of the organ of Corti at P6, P10 and P16 in transversal view projection on the *XY axis*. The *lines* indicate the starting level for the projection on the *XZ level* shown on *XX′* of the OC and they are signalled below by *XX′*. *XX′* projection of the organ of Corti on the *XZ* plane. *Arrowheads/Asterisks* represent loss/maintaining of E-cadherin labelling (*red*), respectively. Cell nuclei are stained with DAPI (*blue*). *D*(*1–3*) Deiters' cell, *I* inner hair cell, *Ip* inner pillar cell, *N* Nuel's spaces, *O*(*1–3*) outer hair cell, *Op* outer pillar cell, *P* phalangeal cell, *TC* tunnel of Corti, and *V* spiral vessel. *Bars* 15 μm

Intense expression of cytokeratin in supporting cells at P10-12

A labelling is only obtained with antibodies anti-cytokeratin pan and anti-cytokeratin 8 (Fig. 6a–f). It is similar with both antibodies (unshown results). Only the epithelial cells of the cochlea can exhibit a labelling. No labelling occurs in the cells of mesenchymal origin at all developmental stages examined in this study (Fig. S2). This labelling is in total agreement with previous observations made in rat (Ramaekers et al. 1987). In the OC, only the supporting cells were cytokeratin-positive; the hair cells were never labelled whatever the antibodies used and the developmental stages studied.

In transversal sections between E18 and E21 (Fig. 6a), the dorsal epithelium of the cochlear duct is lightly cytokeratin-positive, specifically the supporting cells. In addition the OC labelling, some cells of the outer sulcus as well as the epithelia of the future Reissner membrane and stria vascularis are also highly positive with these antibodies.

Between E22 and P6 (Fig. 6b), a signal is exclusively found in the supporting cells, particularly the phalangeal cell at their lateral edges, near to their apical surfaces, which are in contact with their inner hair cells and their inner pillar cells. The cells of outer sulcus are also cytokeratin-positive.

Between P8 and P12 (Fig. 6c–e), an intense labelling is present in the cochlear duct. All the supporting cells are labelled but in a lesser extent the pillar cells. On the other hand, the labelling decreases strongly in the outer sulcus cells.

From P14 to P25 (Fig. 6f), although much weaker, the fluorescent signal is present in the supporting cells at their baso-lateral surfaces.

Discussion

Local loss of adhesion between supporting cells of the OC from P8

Our results indicate clearly that the cell adhesion molecule, E-cadherin, is preferentially found in the lateral membranes of the cells situated in the external part of the OC from E18 to P25. This observation is in good agreement with previous data described in rats (Simonneau et al. 2003) and in mice (Whitlon 1993). We show further that E-cadherin molecules disappear from the lateral cell membranes of pillar and Deiters cells in basal turn of cochlea at P8, namely, when fluid spaces—Corti tunnel and Nuel spaces—form in rats. From this moment, E-cadherin molecules are present only on the lateral edges, near to the apical and basal surfaces, of pillar and Deiters cells,

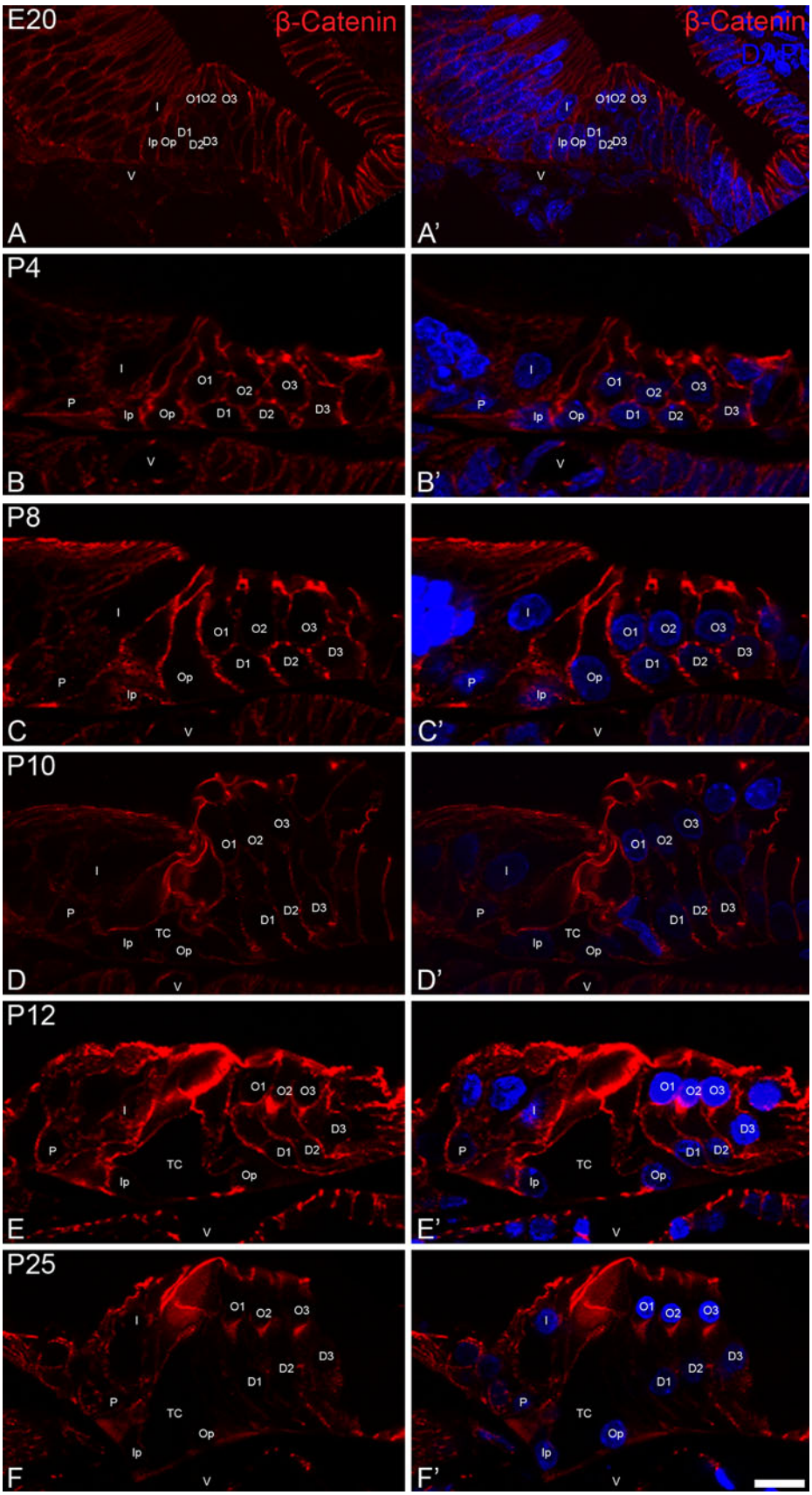

Fig. 4 *β*-catenin immunolabelling within the dorsal epithelium of the cochlear duct from E21 to P25. **a**–**f** Immunolocalization of the *β*-Catenin (*red*). **a**′–**f**′ Merged image with cell nuclei stained with DAPI (*blue*). *D*(*1–3*) Deiters' cells, *Ip* inner pillar cell, *I* inner hair cell, *N* Nuel's spaces, *O*(*1–3*) outer hair cell, *Op* outer pillar cell, *P* phalangeal cell, *TC* tunnel of Corti, *V* spiral vessel. *Bar* 10 μm

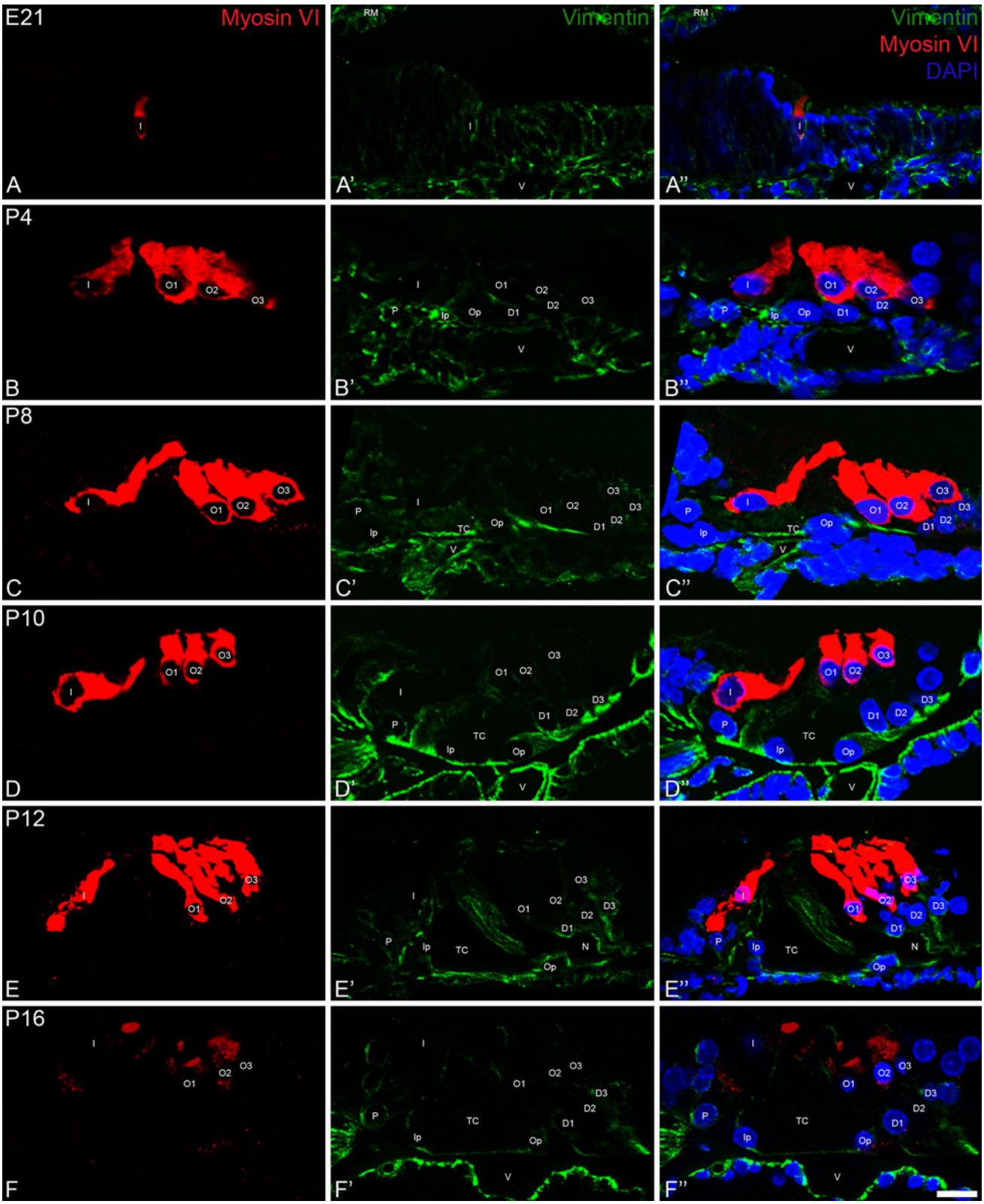

Fig. 5 Vimentin immunolabelling within the dorsal epithelium of the cochlear duct from E21 to P16. **a**–**f** Localization of the hair cells using Myosin VI (*red*). **a′**–**f′** Immunolocalization of the vimentin (*green*). **a″**–**f″** Merged image with cell nuclei stained with DAPI (*blue*). *D*(*1*–*3*) Deiters' cells, *Ip* inner pillar cell, *I* inner hair cell, *N* Nuel's spaces, *O*(*1*–*3*) outer hair cell, *Op* outer pillar cell, *P* phalangeal cell, *TC* tunnel of Corti, *V* spiral vessel. *Bar* 10 μm

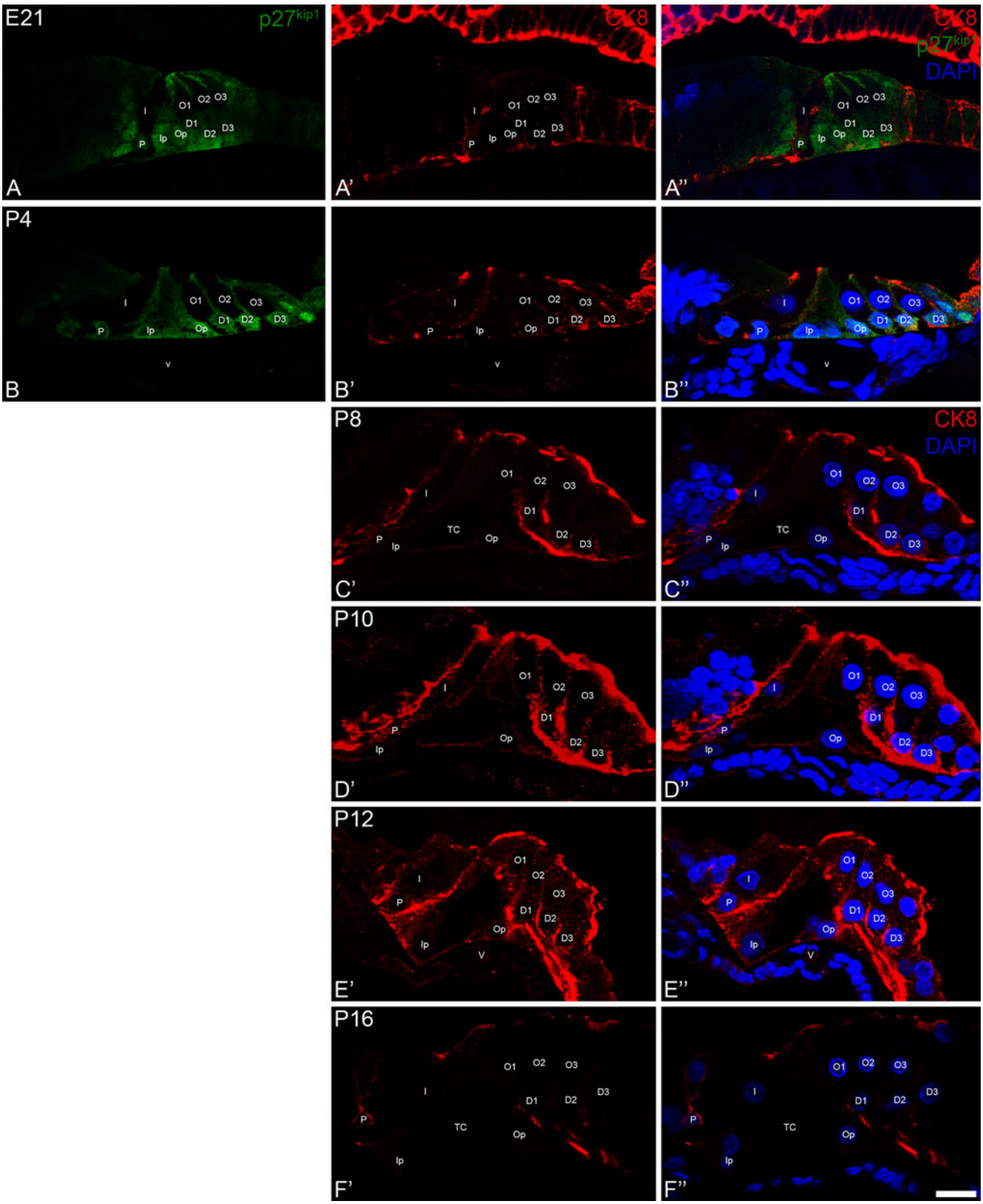

Fig. 6 Cytokeratin 8 immunolabelling within the dorsal epithelium of the cochlear duct from E21 to P16. **a**–**b** Localization of the supporting cells using $p27^{kip1}$ (*green*). **a′**–**f′** Immunolocalization of the cytokeratin 8 (*red*). **a″**–**f″** Merged image with cell nuclei stained with DAPI (*blue*). *D*(*1*–*3*) Deiters' cells, *Ip* inner pillar cell, *I* inner hair cell, *N* Nuel's spaces, *O*(*1*–*3*) outer hair cell, *Op* outer pillar cell, *P* phalangeal cell, *TC* tunnel of Corti, *V* spiral vessel. *Bar* 10 μm

particularly at their connections. The absence of E-cadherin in the internal membranes of pillar cells which will face the opening of the Corti tunnel had already been noted at P7 in mouse (Whitlon 1993). Such observation had never been reported in rat because the distribution of E-cadherin has not been studied systematically during the postnatal development (Simonneau et al. 2003). However, a loss of E-cadherin-linked molecule β-catenin between the pillar cells had been observed at P6 in rat (Simonneau et al. 2003). We also show that the β-catenin labelling reduces strongly on the lateral cell membranes of pillar and Deiters cells in basal turn of cochlea from P12, suggesting that the loss of cadherin molecules occurs before that of β-catenin molecules.

Increased expression of cytokeratins in supporting cells around P10

Contrary to the actin microfilaments and microtubules cytoskeleton, intermediate filaments have distinct tissue-specific functions (Eriksson et al. 2009). Hence, in the epithelial cells, a highly diverse group of cytokeratins is expressed. Our results reveal that cytokeratins are only detected in supporting cells, but not in sensory cells, of the OC epithelium from E18 to P25. We also show that only cytokeratins typical for simple epithelium labelled the OC. These results are in agreement with previous data obtained in rat during some developmental stages (Kuijpers et al. 1991a, b, 1992) and in other adult mammal species (Mogensen et al. 1998; Arnold and Anniko 1990; Sakuma 1998).

An interesting observation is the increase of labelling in the supporting cells around P10, shortly after the beginning of the opening of the Corti tunnel and Nuel spaces. Later, the labelling decreases and becomes essentially limited to the basal and apical areas of supporting cells. The increase of cytokeratin expression around P10 might be in relation with the development of structural and mechanical integrity of supporting cells just after the opening of the fluid spaces and the increase in height of the OC. One might also ask whether the profound morphological changes might also induce the increase of cytokeratin expression. Indeed, it is well known that intermediate filament levels increase dramatically in response to stress and that, in addition to their primary role in cell plasticity, intermediate filaments also function as highly specialised cytoskeletal stress proteins that promote cellular organization and homeostasis (Herrmann et al. 2009; Toivola et al. 2010).

Temporary appearance of vimentin in supporting cells at P8–10

Although vimentin is not an intermediate filament protein typical for the epithelial cells but it is a marker for the mesenchymal cells (Eriksson et al. 2009), we show in this study the presence of vimentin in supporting cells and not in hair cells in the OC from E18 to P25. The presence of vimentin in the OC has rarely been reported during its development (Kuijpers et al. 1992) but it has been repeatedly described in adult in pillar and Deiters cells (Oesterle et al. 1990; Bauwens et al. 1991). However, at P25 we do not observe vimentin in the OC. This is in agreement with a previous study realised on rat at P40 (Kuijpers et al. 1992). The temporary appearance of vimentin between P8 and P10 is not limited to the supporting cells bordering on the fluid spaces but involved all the supporting cells including phalangeal cells. This result seems to indicate that this temporary appearance of vimentin in the OC is not directly involved in the formation of fluid spaces but could have a more general role in the postnatal development of the OC. It is also interesting to note that mice lacking vimentin developed and reproduced without an obvious phenotype (Colucciguyon et al. 1994). Furthermore, no compensatory expression of another intermediate filament could be demonstrated (Colucciguyon et al. 1994). Complementary studies on this mice mutant are now required to better understand the role of vimentin in OC development.

Evidence of a partial EMT in postnatal morphogenesis of the OC

It is well known that the EMT plays crucial role in the differentiation of multiple tissues and organs (Thiery et al. 2009; Savagner 2010), in particular the development of the semicircular canals (Kobayashi et al. 2008). However, no EMT has been described to date in the development of the auditory organ. EMT involves the formation of motile cells from parent epithelial cells that are not themselves motile (Zeisberg and Neilson 2009). This change is accompanied by loss of cell adhesion and the appearance of markers typical of mesenchymal cells, such as vimentin (Yilmaz and Christofori 2009; Zeisberg and Neilson 2009; Savagner 2010). In this work, we show a loss of cell adhesion in the OC. However, only the membrane surfaces in contact with the fluid spaces lose their E-cadherin molecules. A previous study also revealed the appearance of T-cadherin molecules in pillar cells lining the tunnel of Corti after birth (Simonneau et al. 2003). T-cadherin is expressed in cells sharing a mesenchymal phenotype (Riou et al. 2006; Simonneau et al. 2003). Our results show further that this reduction in cell adhesion is accompanied by an increased expression of vimentin, a marker characteristic of mesenchymal cells (Zeisberg and Neilson 2009). Curiously, this increased expression of vimentin is not concomitant with a reduction in the expression of cytokeratins, a marker typical of epithelial cells, as generally described for EMT (Savagner 2010). All these results clearly suggest that a

partial EMT could be involved in the remodelling of the OC during postnatal development in rat. The EMT would occur at a critical time during development of the Corti organ. Indeed, it is between P8 and P12 in rat that occur deep morphological changes of the Corti organ, including the formation of fluid spaces and the increase in height of the epithelium. At P12 in rat, the OC is considered to be functional even if its maturation continues until P25 (Savagner 2010). Further studies are now needed to identify the molecular factors responsible for the implementation of the EMT.

Acknowledgments The authors thank Mrs. Patricia Piscicelli for her skilful technical assistance. They would like also to thank Sandra Ormenese (GIGA-Imaging and Flow Cytometry, University of Liège) and Dr Pierre Leprince (Western blots, University of Liège) for their technical supports. This work was supported by the Fonds de la Recherche Scientifique and the Recherche dans l'Industrie et dans l'Agriculture.

References

Arnold W, Anniko M (1990) The cytokeratin skeleton of the human organ of Corti and its functional significance. Laryngo-rhino-otologie 69(1):24–30

Bauwens L, Veldman JE, Ramaekers FCS, Bouman H, Huizing EH (1991) Expression of intermediate filament proteins in the adult human cochlea. Ann Otol Rhinol Laryngol 100(3):211–218

Chen P, Segil N (1999) p27kip1 links cell proliferation to morphogenesis in the developing organ of Corti. Development 126:1581–1590

Colucciguyon E, Portier MM, Dunia I, Paulin D, Pournin S, Babinet C (1994) Mice lacking vimentin develop and reproduce without an obvious phenotype. Cell 79(4):679–694

Eriksson JE, Dechat T, Grin B, Helfand B, Mendez M, Pallari HM, Goldman RD (2009) Introducing intermediate filaments: from discovery to disease. J Clin Invest 119(7):1763–1771

Herrmann H, Strelkov SV, Burkhard P, Aebi U (2009) Intermediate filaments: primary determinants of cell architecture and plasticity. J Clin Invest 119(7):1772–1783

Kalluri R, Weinberg RA (2009) The basics of epithelial-mesenchymal transition. J Clin Invest 119(6):1420–1428

Kelley MW (2006) Regulation of cell fate in the sensory epithelia of the inner ear. Nat Rev Neurosci 7(11):837–849

Kelley MW (2007) Cellular commitment and differentiation in the organ of Corti. Int J Dev Biol 51(6–7):571–583

Kelley MW, Driver EC, Puligilla C (2009) Regulation of cell fate and patterning in the developing mammalian cochlea. Curr Opin Otolaryngol Head Neck Surg 17(5):381–387

Kim K, Daniels KJ, Hay ED (1998) Tissue-specific expression of beta-catenin in normal mesenchyme and uveal melanomas and its effect on invasiveness. Exp Cell Res 245(1):79–90

Kobayashi Y, Nakamura H, Funahashi JI (2008) Epithelial-mesenchymal transition as a possible mechanism of semicircular canal morphogenesis in chick inner ear. Tohoku J Exp Med 215(3):207–217

Kuijpers W, Peters TA, Tonnaer E, Ramaekers FCS (1991a) Expression of cytokeratin polypetptides during development of the rat inner-ear. Histochemistry 96(6):511–521

Kuijpers W, Tonnaer E, Peters TA, Ramaekers FCS (1991b) Expression of intermediate filaments proteins in the mature inner-ear of the rat and guinea-pig. Hear Res 52(1):133–146

Kuijpers W, Tonnaer E, Peters TA, Ramaekers FCS (1992) Developmentally-regulated coexpression of vimentin and cytokeratins in the rat inner-ear. Hear Res 62(1):1–10

Mogensen MM, Henderson CG, Mackle JB, Lane EB, Garrod DR, Tucker JB (1998) Keratin filament deployment and cytoskeletal networking in a sensory epithelium that vibrates during hearing. Cell Motil Cytoskelet 41(2):138–153

Mu MY, Chardin S, Avan P, Romand R (1997) Ontogenesis of rat cochlea. A quantitative study of the organ of Corti. Dev Brain Res 99(1):29–37

Oesterle EC, Sarthy PV, Rubel EW (1990) Intermediate filaments in the inner ear of normal and experimentally damaged guinea pigs. Hear Res 47(1–2):1–16

Osborn M, Debus E, Weber K (1984) Monoclonal antibodies specific for vimentin. Eur J Cell Biol 34(1):137–143

Ramaekers FCS, Huysmans A, Schaart G, Moesker OPV (1987) 5. Cytoskeletal proteins as markers in surgical pathology. In: Ruiter DJ, Fleuren GF, Warnaar SO (eds) Application of monoclonal antibodies in tumor pathology Martinus Nijhoff Publishers. Dordrecht, Boston, pp 65–85

Riou P, Saffroy R, Chenailler C, Franc B, Gentile C, Rubinstein E, Resink T, Debuire B, Piatier-Tonneau D, Lemoine A (2006) Expression of T-cadherin in tumor cells influences invasive potential of human hepatocellular carcinoma. Faseb J 20(13):2291–2301

Roth B, Bruns V (1992a) Postnatal-development of the rat organ of Corti. 1. General morphology, basilar-membrane, tectorial membrane and border cells. Anat Embryol 185(6):559–569

Roth B, Bruns V (1992b) Postnatal-development of the rat organ of Corti. 2. Hair cell receptors and their supporting elements. Anat Embryol 185(6):571–581

Sakuma H (1998) Regional variations of the cytokeratin expression along the guinea pig cochlear turn. Nihon Jibiinkoka Gakkai kaiho 101(11):1348–1357

Sato M, Leake PA, Hradek GT (1999) Postnatal development of the organ of Corti in cats: a light microscopic morphometric study. Hear Res 127(1–2):1–13

Savagner P (2010) The epithelial-mesenchymal transition (EMT) phenomenon. Ann oncol Off J Eur Soc Med Oncol/ESMO 21(Suppl 7):vii89–vii92

Simonneau L, Gallego M, Pujol R (2003) Comparative expression patterns of T-, N-, E-cadherins, beta-catenin, and polysialic acid neural cell adhesion molecule in rat cochlea during development: Implications for the nature of Kolliker's organ. J Comp Neurol 459(2):113–126

Thelen N, Breuskin I, Malgrange B, Thiry M (2009) Early identification of inner pillar cells during rat cochlear development. Cell Tissue Res 337(1):1–14

Thiery JP, Acloque H, Huang RY, Nieto MA (2009) Epithelial-mesenchymal transitions in development and disease. Cell 139(5):871–890

Toivola DM, Strnad P, Habtezion A, Omary MB (2010) Intermediate filaments take the heat as stress proteins. Trends Cell Biol 20(2):79–91

Whitlon DS (1993) E-Cadherin in the mature and developing organ of Corti of the mouse. J Neurocytol 22(12):1030–1038

Wikstrom SO, Anniko M, Thornell LE, Virtanen I (1988) Developmental stage-dependent pattern of inner ear expression of intermediate filaments. Acta Otolaryngol 106(1–2):71–80

Yilmaz M, Christofori G (2009) EMT, the cytoskeleton, and cancer cell invasion. Cancer Metastasis Rev 28(1–2):15–33

Zeisberg M, Neilson EG (2009) Biomarkers for epithelial-mesenchymal transitions. J Clin Invest 119(6):1429–1437

Zhang L, Hu Z (2012) Sensory epithelial cells acquire features of prosensory cells via epithelial to mesenchymal transition. Stem Cells and Development [Epub ahead of print]